Subassemblage Test of Continuously Buckling Restrained Braced RC Frames

Y. Maida, Z. Qu, H. Sakata & A. Wada
Tokyo Institute of Technology,Tokyo

S. Kishiki
Osaka Institute of Technology,Osaka

T. Maegawa & M. Hamada
Kumagai Gumi Co., Ltd., Tokyo

SUMMARY:
Cyclic loading test of subassemblies of continuously buckling restrained braced RC frames is conducted to evaluate the behavior of the connection details of BRBs and its influence on the surrounding RC components. Each subassembly consists of a RC beam-to-column joint with two columns (lower and upper stories), a beam framing into it and a set of BRBs that are diagonally connected to the beam-to-column joint. To achieve necessary boundary conditions, the specimen is rotated 90 degrees and is loaded with two displacement-controlled horizontal actuators at the column bottom and the beam end. It was observed that for all the specimens, BRBs yield and start to dissipate energy at an early stage with story drift ratios much smaller than those at beam yielding. The concrete corbels and the pre-stressing anchor bolts provide not only sufficient strength but also large stiffness to minimize the deformation loss in the BRB connections.

Keywords: buckling restrained braced frame, reinforced concrete, subassemblage test

1. INTRODUCTION

In Recent years, applications of BRBs in reinforced concrete (RC) frames have attracted much attention, in which, the connection of BRBs to RC frames is important. However, there are not commonly accepted details of installing BRBs on RC frames. The authors suggested a continuously buckling restrained braced frame system in which the BRBs are arranged in the form of a Warren truss (Maida et al, 2011). The corresponding BRB connection detail in the proposed system, which consists of anchor bolts and RC corbels, has been confirmed effective through component tests and subassemblage tests with BRBs simulated by force-controlled jacks (Qu et al, 2011). However, some other important issues, such as the performance of the BRBs in the proposed system, need to be investigated. To do this, subassemblies consisting of RC beam, column and BRBs of the proposed system were subjected to cyclic loading. The major parameter of this test investigation was the proportion of the yield strength of the BRBs in the upper and the lower stories. This experiment confirmed the influence of the unbalanced BRB force in the upper and the lower stories on the performance of the BRB connection.

2. EXPERIMENTAL PROGRAM

The specimens were 1/2 scale RC beam and column subassemblies with BRBs that resembles the trial design of a high-rise RC building (Kikuta et al, 2010). The details of the specimens are shown in Fig. 2.1 and 2.2. Specimen properties are shown in Table 2.1. For each specimen, BRBs in the upper and the lower stories were attached to the beam-to-column joint through a single gusset plate. The inclination angle of the BRBs was 40.4 deg. A group of eight anchor bolts fastened the gusset plate to the concrete joint and high strength non-shrink grout was filled between the gusset plate and the two RC corbels projecting from the column. Mortar filled steel tubes were used to restrain the buckling of the core of the BRBs (Fujimoto et al, 1988).

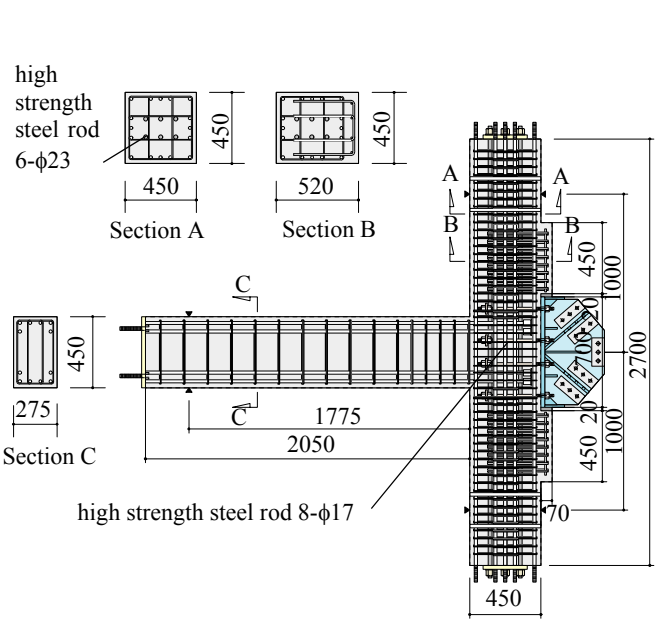

Figure 2.1. Details of specimens

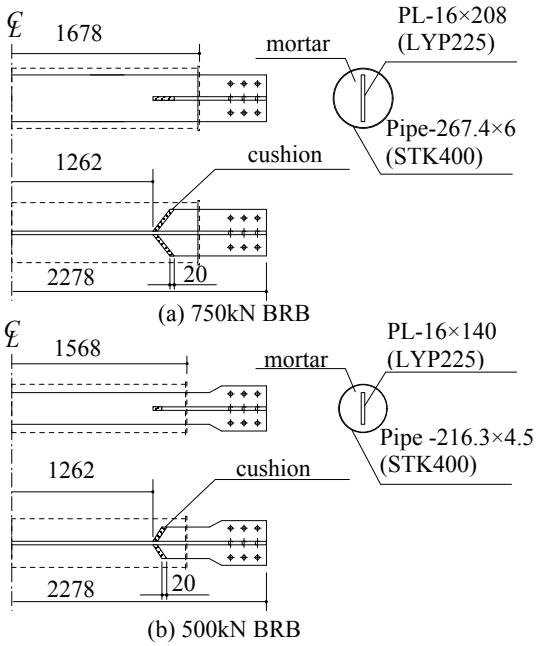

Figure 2.2. Details of BRBs

Table 2.1. Specimen Specifications

	75-75N	50-75N	0-75N	0-75S
Beam dimensions (mm)	275×450			
Beam longitudinal rebar	6-D19			
Stirrups in corbels	D10@50 - 8 legs			
Pre-tension per bolt (PC rod6-ϕ23) (kN)	571.2	571.2	571.2	0
Column dimensions (mm)	450×450			
Column longitudinal rebar	12-D19			
Column hoop	D10@70 - 4 legs			
Beam stirrup	D10@70 - 2 legs			
Yield strength of upper BRB (kN)	750	500	0	0
Yield strength of lower BRB (kN)	750	750	750	750
Presence of strut	no	no	no	yes

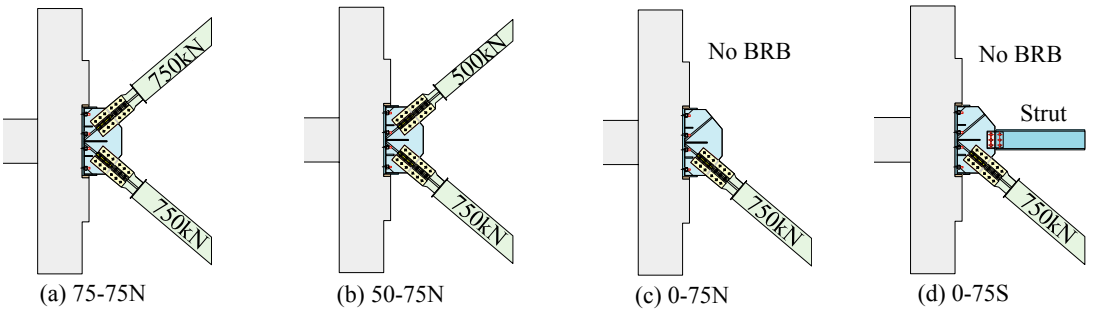

(a) 75-75N (b) 50-75N (c) 0-75N (d) 0-75S

Figure 2.3. Configuration of BRBs and strut

The major difference among the specimens was in the proportion of the yield strengths of the BRBs in the upper and the lower stories, and in the mechanism of resisting the horizontal force on the gusset plate. Four specimens were tested. These were '75-75N' of 750 kN BRBs for both the upper and the lower story; '50-75N' of a 500 kN BRB in the upper and a 750 kN BRB in the lower story, which resembled the case for a middle story of a high-rise building where the yield strength of the BRBs is changed; '0-75N' of only a 750 kN BRB in the lower story, which resembled the top story of a building. In the above three specimens, the anchor bolts for fastening the gusset plate was pre-tensioned to increase the stiffness of the connection. In the fourth specimen, namely '0-75S' in

which only a 750 kN BRB was installed in the lower story, the anchor bolts were not pre-tensioned. Instead, a steel strut was installed to help resisting the horizontal force on the gusset plate (see Fig. 2.3).

High strength steel rods of 17 mm diameter were used for the anchor bolts. For each of the first three specimens, the group of eight steel rods was prestressed to provide 571.2 kN pre-tension, which equals the horizontal component of the yield strength of a single 750kN BRB, that is, $P_y \cos\alpha$, where P_y is the yield strength and α is the inclination angle of the BRB. In other words, each anchor bolt in the group was prestressed to 71.4 kN.

The test setup is shown in Fig. 2.4 and Photo 2.1. The specimen was rotated 90 degrees clockwise. The top and the bottom of the column were supported by pin rollers that allow for horizontal movement. The beam was restrained at its free end by two actuators in its axial direction. The bottom of the column and the beam free end were driven by two horizontal displacement-controlled jacks to impose deformation to the specimen.

The displacement of the two horizontal jacks kept a certain proportion during the loading. When the

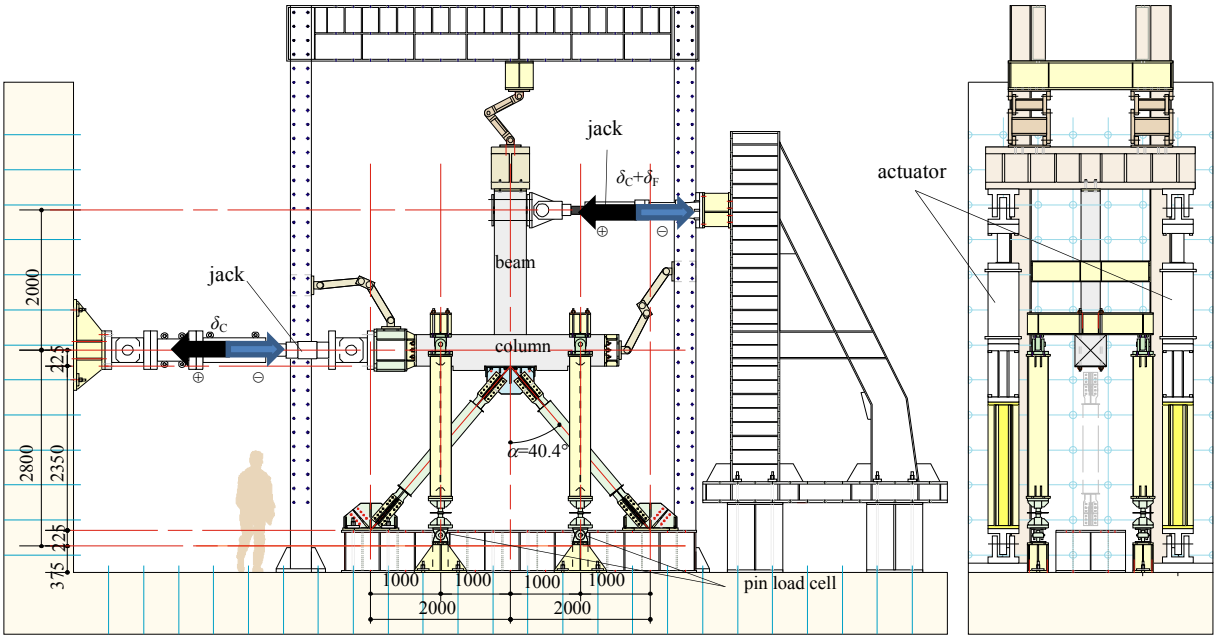

Figure 2.4. Experimental setup

Photo 2.1. Experimental setup

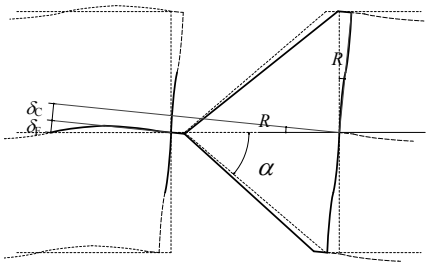

Figure 2.5. Deformation of building

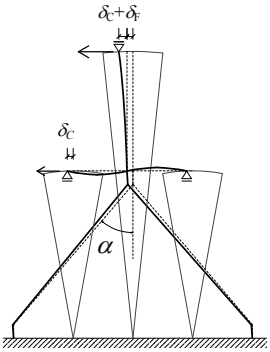

Figure 2.6. Deformation in experiment

column was displaced by δ_C, resulting in a story drift ratio R, the beam end should be displaced by $\delta_C+\delta_F$ in order to create the deformation pattern as shown in Fig. 2.5. The two vertical actuators were also displacement-controlled to exhibit zero displacement during the test. Cyclic loading with increasing displacement amplitudes was conducted. For each specimen, two cycles were carried out for story drift ratio amplitudes of 1/1600, 1/800, 1/400, 1/200, 1/100. After that, only one cycle was carried out for amplitudes of 1/50 and 1/33.

3. EXPERIMENTAL RESULTS

3.1. Global response

The crack patterns at story drift ratio R = -1/100 of all specimens are shown in Fig. 3.1. For all specimens, flexural cracks occurred on the beam ends at an early stage. Afterwards, flexural-shear cracks accompanied the increase of the story drift ratio. The longitudinal rebar of beam yielded at R = 1/120 for the '75-75N' specimen, and shear cracks were observed at R = 1/100 on the beam-to-column joint.

The story drift ratio versus shear force relationship of the '75-75N' specimen is shown in Fig. 3.2(a). The story shear force can be separated into two parts, that is, the contribution of the RC part in the subassembly, Q_F, and that of the BRBs, which is directly related to the axial force of the BRBs, N_{BRB}. The hysteresis of the RC part and the BRB in the lower story is shown in Fig. 3.2(b) and (c). Compressive force was acted on the beam in positive loading because of the difference in the yield strength of the upper and the lower BRBs for '50-75N', '0-75N' and '0-75S' specimens. As a result, the yield strength of the beam was a little bit increased for these specimens.

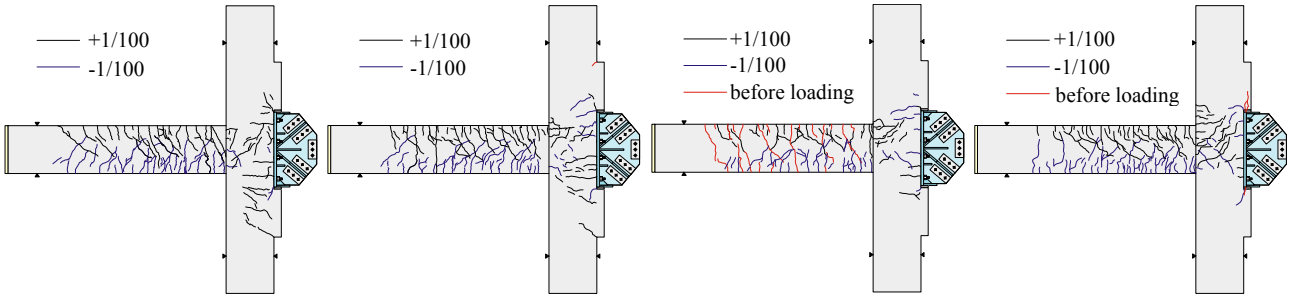

(a) 75-75N (b) 50-75N (c) 0-75N (d) 0-75S

Figure 3.1. Cracks of RC part at R=+1/100 and R=-1/100

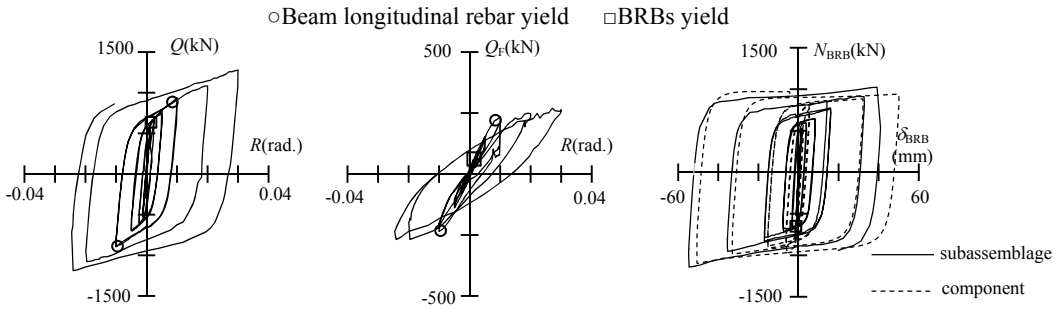

(a) subassemblage (b) RC part (c) BRBs

Figure 3.2. Behavior of '75-75N' specimen

The accumulative hysteretic energy dissipation of the RC part, W_F, and that of the upper BRB, W_{DU}, and the lower BRB, W_{DL}, for '75-75N' specimen are shown in Fig. 3.3. At R = -1/100, the energy dissipated by the lower BRB, W_{DU} = 98.6kNm, by the upper BRB, W_{DD} = 96.0kNm, and by the RC part, W_F = 9.2kNm. It is evident that the BRBs are very effective in dissipating energy in a RC frame

by the fact that the energy dissipation in each BRB was approximately 10 times that in the RC part. Only the results for '75-75N' specimen is shown here as an example. Similar observations were made for all the other specimens.

The development of the crack width of the beam of '75-75N' specimen is shown in Fig. 3.4. The crack width was measured on the beam surface at the projecting position of the longitudinal rebars. The total and the maximum width is the sum and the maximum of the width of all the cracks on the beam surface going through the longitudinal rebars, respectively. For all the specimens, the total crack width was about 2 mm and the maximum one was about 0.2 mm at R = -1/100.

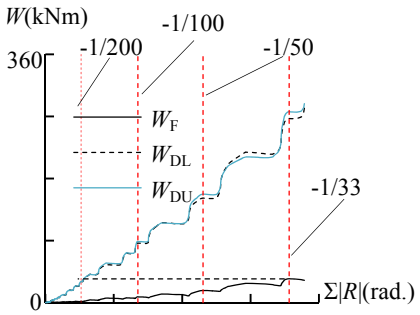

Figure 3.3. Hysteretic energy dissipation

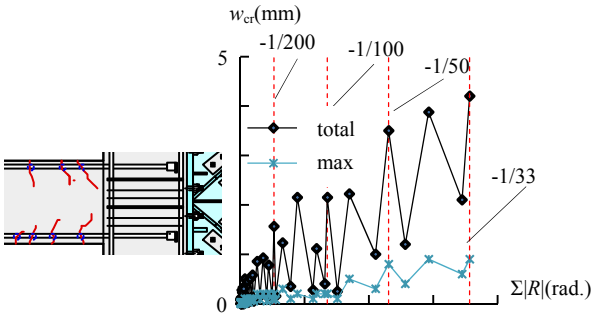

Figure 3.4. Crack width on beam

3.2. Behavior of BRBs

The axial deformation of BRBs measured in the experiment is compared with the ideal work point-to-work point deformation calculated from the story drift ratio (Eqn. 3.1) in Fig. 3.5. The latter can be regarded as a maximum deformation a BRB should be able to sustain if the connection is rigid. In the experiment, however, it was observed for '0-75N' and '0-75S' specimens that the measured axial deformation of the BRB was only 40 ~ 50% of the ideal displacement when the deformation of the subassembly was small, for example, the story drift ratio is less than 1/400. When the story drift ratio became larger, the ratio of the measured BRB deformation and the ideal brace displacement

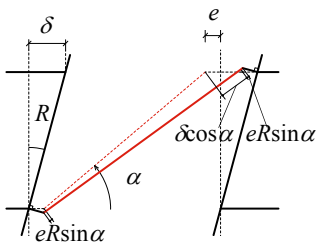

(a) work point-to-work point deformation calculated

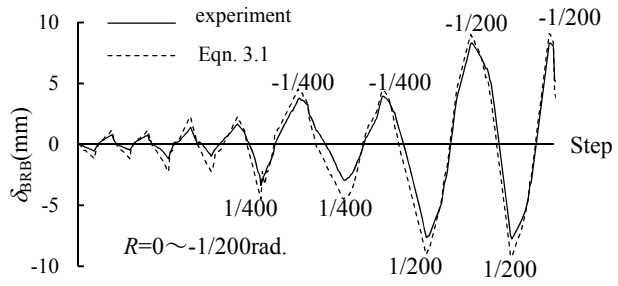

(b) Comparison between experiment and Eqn. 3.1

Figure 3.5. Axial deformation of BRBs '75-75N'

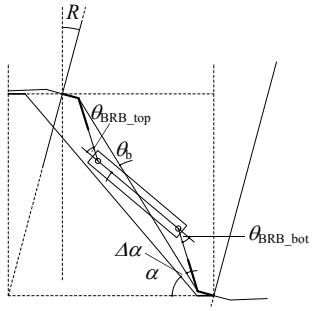

(a) plastic rotations at both ends calculated

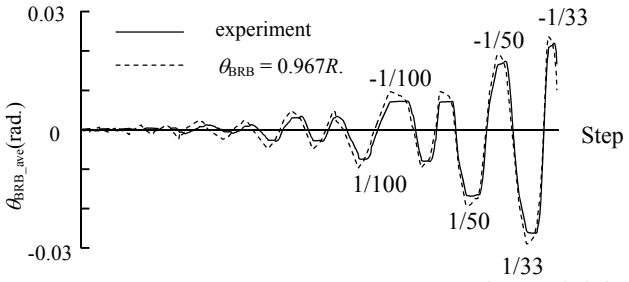

(b) Comparison between experiment and $\theta_{BRB} = 0.967R$.

Figure 3.6. Rotation of BRB end of '75-75N' specimen

increased significantly. It is no less than 90 % for story drift ratio greater than 1/200 for all the specimens.

$$\delta_{\mathrm{BRB}} = \delta \cos\alpha + 2eR \sin\alpha \tag{3.1}$$

where e is eccentricity of the BRB work point with respect to the column and beam centerlines.

Different from component test of a single BRB subjected to uniaxial loading, the BRBs in the subassembly test sustained obvious plastic rotations at both ends (Fig. 3.6(a)). The measured end rotation is shown in Fig. 3.6(b). The rotation $\theta_{\mathrm{BRB\_ave}}$ is taken as the average of $\theta_{\mathrm{BRB\_top}}$ and $\theta_{\mathrm{BRB\_bot}}$ as shown in Fig. 3.6(a). It increased with the increase of the story drift ratio of the subassembly. This rotation can be estimated by the equation proposed by Kozai Club. (1998) from the story drift ratio R. For the present test, $\theta_{\mathrm{BRB}} = 0.967R$. The estimated rotation is compared with the measured one in Fig. 3.6(b).

3.3. Behavior of BRB connection

The relationship of the horizontal displacement of the gusset plate, δ_{H}, versus the horizontal force on the gusset plate, P_{DH} (see Fig. 3.7), for '0-75N' and '0-75S' specimens are compared in Fig. 3.8. The tensile force on the gusset plate of the two specimens was almost the same. Notwithstanding, the maximum horizontal displacement of '0-75S' specimen was about 1.1 mm in both the pulling and the pushing direction, while that of '0-75N' specimen was only about 0.25 mm in the pulling and negligible in the pushing direction. The pre-tension of the anchor bolts seems more effective than installing a strut for resisting the tensile force on the gusset plate.

The relationship of the vertical displacement of the gusset plate, δ_{V}, versus the shear force on the gusset plate, P_{DV}, for '0-75N' and '0-75S' specimens are compared in Fig. 3.9. The vertical displacement δ_{V} is taken as the average of δ_{VU} and δ_{VL} as shown in Fig. 3.7. The possible friction force between the gusset plate and the underneath concrete in '0-75N' specimen is also shown as dashed lines in the figure, assuming a coefficient of friction of 0.4 (AIJ, 2011). For the '0-75N' specimen, the gusset plate has no vertical displacement until the shear force exceeds the friction force and the corbel begins to carry the extra shear force. As a result, the shear force carried by the corbel in the '0-75N' specimen was much smaller than that in the '0-75S' specimen, where there was much less friction force on the gusset plate-to-concrete interface. Accordingly, the shear deformation, δ_{V}, in the '0-75N' specimen is much smaller than that in the '0-75S' specimen during the positive loading, as can be seen in Fig. 3.9. In this sense, the pre-tensioning of the anchor bolts also has an effect on the shear resistance of the BRB connection.

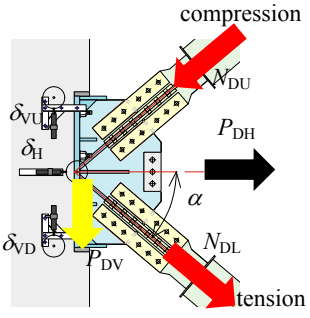

Figure 3.7. Location of displacement transducers

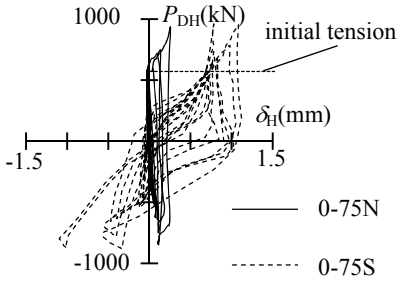

Figure 3.8. Horizontal displacement of gusset plate - tension of gusset plate relations

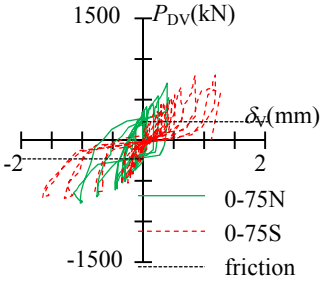

Figure 3.9. Vertical displacement of gusset plate - shear force of gusset plate relations

4. CONCLUSIONS

In this study, cyclic test of the subassemblies of continuously buckling restrained braced RC frame

was conducted. It is confirmed by the test results that both the RC frame and the BRBs in the system exhibit stable hysteretic behavior. In addition, the performance of the horizontal resistance of the BRB connection was investigated. It seems more effective to introduce initial tension into the anchor bolts to resist the horizontal force than to install a steel strut.

AKCNOWLEDGEMENT

This work was supported by the Grants-in-Aid for Scientific Research (A) (22246070). Part of the experimental results represented in this paper is a part of a research project entitled 'Feasibility of applying buckling restrained braces in high-rise residential buildings' sponsored by Kumagai Gumi Co., Ltd.

REFERENCES

Maida, Y, Qu, Z, Kishiki, S, Sakata, H, Wada, A, et al. (2011). Applications of buckling restrained braces in reinforced concrete frames. *Summaries of technical papers of AIJ annual meeting.* **C-2**:667-678.

Qu, Z, Maida, Y, Nonoyama, M, Kishiki, S, Sakata, H, Wada, A. (2011), Hybrid control test of connections for buckling restrained braces in RC continuously braced frames, *Proc. 4th Intl. Conf. on Advances in Experimental Structural Engineering*, Italy, in CD-ROM.

Kikuta, S, Hamada, M, et al. (2010), "Structural Performance of RC High-rise Buildings under Long Period Seismic Ground Motion : Part 10 Experimental study on the beam column sub-assemblages with different safety margin coefficient of bond and shear, "*Summaries of technical papers of AIJ annual meeting*, **C-2**:729-730.

Fhjimoto, M, Wada, A, Saeki, E, Watanabe, A, Hitomi, Y. (1988). A study on the unbonded brace encased in buckling-restraining concrete and steel tube. *Journal of Structural Engineering.* **Vol.35B: Architectural Institute of Japan**,249-257.

Kozai Club. (1998). The earthquake response and Seismic Design Method of Steel Frames with Hysteretic Dampers, Japanese Society of Steel Construction

Architectural Institute of Japan. (2011). Stress transferring mechanism and resistance mechanism of steel-reinforced concrete joints, Architectural Institute of Japan